The Influence of Cooling Air Ejection on Flow Development and Heat Transfer in a Rotating Leading Edge Coolant Duct of a Film-Cooled Turbine Blade

Martin Elfert
German Aerospace Center
Institute of Propulsion Technology
D-51170 Cologne, Germany
Fax Number: +49 2203 64395
E-mail address: martin.elfert@dlr.de

Abstract

With increasing turbine inlet temperature, the cooling of gas turbine components exposed to the hot gas flow will be of great importance. The improvement of the efficiency demands higher performance from the blade cooling systems with minimized coolant flow rates to cope with the increase in heat load as well as to meet the obligatory safety requirements. This calls for very accurate knowledge of the gas and coolant side flow and heat transfer, which both affect the blade temperature field, in order to obtain an efficient cooling design.
This paper provides information about rotational effects on fluid motion and heat transfer within a rotating coolant duct of circular cross section with bleeding of cooling air through a row of film cooling holes for the purpose of film cooling of the hot gas side of the blade. Experimental data were obtained from a model mounted to the rotating duct facility at DLR. Flow development were measured by a non-intrusive optical Laser velocimeter. Wall temperature distributions around the duct wall and the generated heat were measured to provide data for local heat transfer analysis. The direction of bleeding is varied against the direction of rotation to study its effect on the development of secondary vortex structures which are generally caused within the flow by the rotational forces. Depending on the direction of bleeding, secondary vortex motion as well as heat transfer variation around the duct circumference are enhanced with pressure side ejection or weakened with suction side ejection.

Nomenclature

d	Duct diameter, mm	Re_{rot}	Rotational Reynolds number, $\rho\Omega d^2/\mu$
E	Relative eccentricity, *e/d*, dimensionless	Ro	Rotation number, $\Omega d/u_b$, dimensionless
e	eccentricity (radius) at mid span, mm	r	Radius, mm
Gr	Grashof number, $\Omega^2 e d^3 \rho \Delta\rho/\mu^2$	T	Temperature, K
k	Kinetic energy of turbulence, m^2/s^2	Tu	Turbulence level, $\sqrt{u'^2}/u_b$, dimensionless
l	Duct length, mm	u,v,w	Velocity in x, y, z-direction, m/s
R	Duct radius, m	x	Streamwise coordinate
Re	Reynolds number, $\rho u_b d/\eta$, dimensionless		

Greek Symbols

ε	Dissipation rate of k, m^2/s^3	ρ	Density, kg/m^3
φ	Circumferential angle, deg	Ω	Angular velocity, s^{-1}
μ	Dynamic viscosity, kg/ms		

Subscripts

PS	Pressure side	b	Bulk (mean value)
SS	Suction side	rot	Rotational
c	Coolant, cooling	w	Wall

Paper presented at the RTO AVT Symposium on "Advanced Flow Management: Part B – Heat Transfer and Cooling in Propulsion and Power Systems", held in Loen, Norway, 7-11 May 2001, and published in RTO-MP-069(I).

Report Documentation Page

Form Approved
OMB No. 0704-0188

1. REPORT DATE	2. REPORT TYPE	3. DATES COVERED
00 MAR 2003	**N/A**	**-**

4. TITLE AND SUBTITLE	5a. CONTRACT NUMBER
The Influence of Cooling Air Injection on Flow Development and Heat Transfer in a Rotating Leading Edge Coolant Duet of a Film-Cooled Turbine Blade	5b. GRANT NUMBER
	5c. PROGRAM ELEMENT NUMBER
6. AUTHOR(S)	5d. PROJECT NUMBER
	5e. TASK NUMBER
	5f. WORK UNIT NUMBER
7. PERFORMING ORGANIZATION NAME(S) AND ADDRESS(ES) **NATO Research and Technology Organisation BP 25, 7 Rue Ancelle, F-92201 Neuilly-Sue-Seine Cedex, France**	8. PERFORMING ORGANIZATION REPORT NUMBER
9. SPONSORING/MONITORING AGENCY NAME(S) AND ADDRESS(ES)	10. SPONSOR/MONITOR'S ACRONYM(S)
	11. SPONSOR/MONITOR'S REPORT NUMBER(S)

12. DISTRIBUTION/AVAILABILITY STATEMENT
Approved for public release, distribution unlimited

13. SUPPLEMENTARY NOTES
Also see ADM001490, presented at RTO Applied Vehicle Technology Panel (AVT) Symposium held in Leon, Norway on 7-11 May 2001, The original document contains color images.

14. ABSTRACT

15. SUBJECT TERMS

16. SECURITY CLASSIFICATION OF:			17. LIMITATION OF ABSTRACT	18. NUMBER OF PAGES	19a. NAME OF RESPONSIBLE PERSON
a. REPORT	b. ABSTRACT	c. THIS PAGE			
unclassified	**unclassified**	**unclassified**	**UU**	**14**	

Introduction

The lowering of the fuel consumption by increase of the process pressure and temperature is a relevant development aim for gas turbines. The aimed temperatures lie well over the permissible material temperatures of present turbine blade materials. Today turbine entry temperatures of approx. 1800 K can be realized by combustion of the fuel with air surplus, a consistently achieved improvement of the blade cooling and the use of temperature sustainable materials with a permissible material temperature of approx. 1250 K. For blade cooling purpose, the required cooling air is taken from the compressor. With an amount of cooling air mass flow rate current to 25% of the total mass flow rate, a substantial part of the spent work for compression gets lost, because the bypassed cooling air is no more available for the combustion any more and can perform in the turbine only insignificant expansion work. A realization of higher turbine entry temperatures by further increase of the cooling air mass flow rate would mean for the cycle process that a big part of the efficiency improvement achieved by the temperature rise is destroyed by the raised cooling air need again. Therefore, an essential measure to the lowering of fuel consumption is the rise of the efficiency of the blade cooling to enable a saving in cooling air and a better process efficiency or higher hot gas temperatures.
To increase the efficiency with the cooling of the turbine blades, exact knowledge about the influence of the rotation on the fluid motion and the heat transfer is required in the cooling channels of the rotor blade. The flow in the rotating cooling channels is affected by strong centrifugal accelerations which cause a very deformed velocity profile as well as a vortex system with two in the opposite direction turning secondary vortices. These vortices are generated by an imbalance of the acting forces (Coriolis, inertia, pressure field) within the boundary layer causing a flow along the duct wall in circulation direction from the pressure side to the suction side. The secondary vortices produce additional wall friction and transport colder fluid from the core to the duct wall and change substantially the local heat exchange as well as the pressure loss in the overall system about these mechanisms (see ref. [1-4]).
The subject of this research project was to determine the influence of the cooling air ejection from the coolant air flow of a rotor blade on the form of the fluid motion as well as the development of the secondary vortices and to describe the influence on the internal heat transfer at the presence of coolant ejection. The boundary layer structure in the vicinity of holes is naturally affected by bleeding off cooling air. Mass and energy is taken away from the described boundary layer flow and by that from the secondary vortices. According to place and orientation of the ejection in relation to the rotational direction different effects on the vortex motion appear as shown later on.
Further intention was to improve a numerical procedure which enables flow and heat transfer calculation also in such complex flow situation. Because the rotation with strong Coriolis-and centrifugal accelerations as well as the cooling air ejection from the channel massively effects flow and heat transfer, a detailed knowledge and predictableness of these effects is essential for the optimization of cooling systems with respect to the optimal utilization of cooling air.

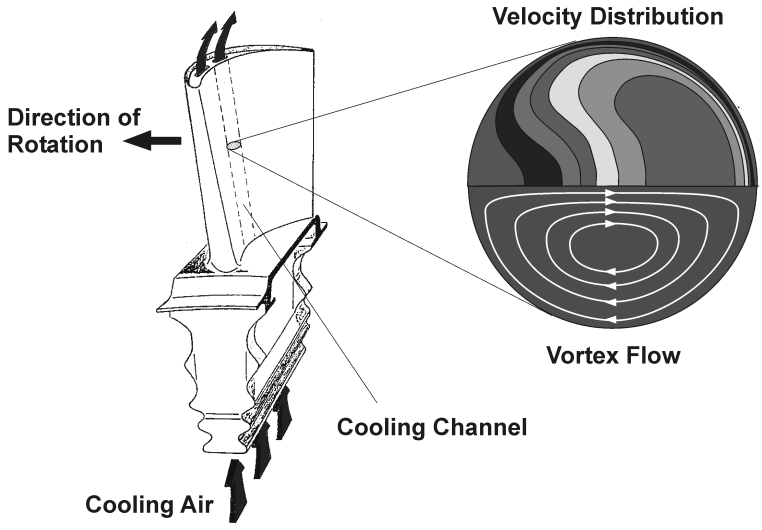

Figure 1: Film-cooled turbine blade and flow field inside rotating coolant passage

A typical film-cooled turbine blade of a high pressure rotor shows Fig. 1. The outlined flow sample within a cooling channel idealized as a tube of circular cross section shows the kidney-shaped deformation of the axial velocity distribution (at the top) as well as the induced streamlines of a vortex (below). The misalignment of the flow core to the duct results from the rotation which causes Coriolis- and centrifugal accelerations in the fluid and results in a change of the pressure field. The Coriolis force decreasing in the boundary layer is not in the balance with the pressure field, so a pressure driven flow is generated from the pressure side to the suction side along both duct sides forming a symmetric vortex pair.

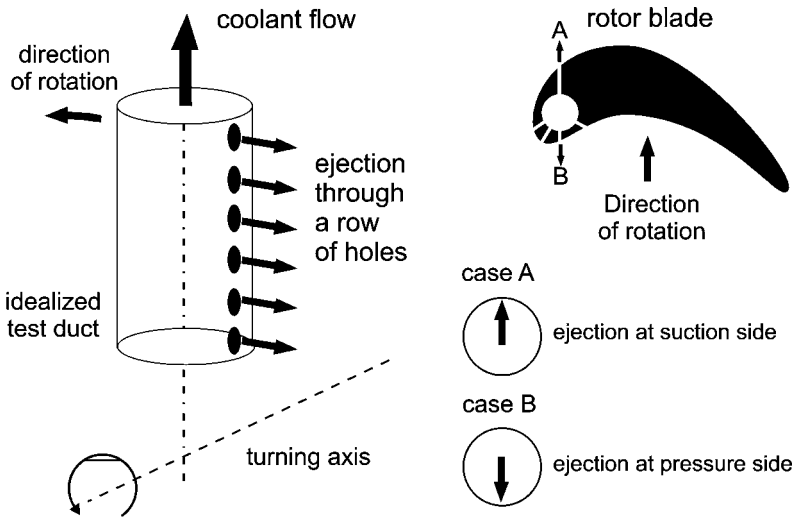

Figure 2: Typical configuration of leading edge film-cooling and analysed ejection positions at pressure side (case A) and suction side (case B)

Fig. 2 shows interesting blowing out positions in comparison to the direction of rotation on the basis of a typical rotor blade. In this paper only the position of blowing out in direction of rotation (φ = 0 deg) and opposite the direction of rotation (φ = 180 deg) is presented.

Description of the experiments

Test facility

A large-scale coolant duct of circular cross-section with one row of film cooling holes rotating spanwise was investigated during the experiments. Air is supplied in the rig through a rotary sealing assembly, a second one is used for venting after the air has passed through the test section. Both are mounted to the end of the double hollow shaft. A schematic of the test rig is given in Fig. 3.

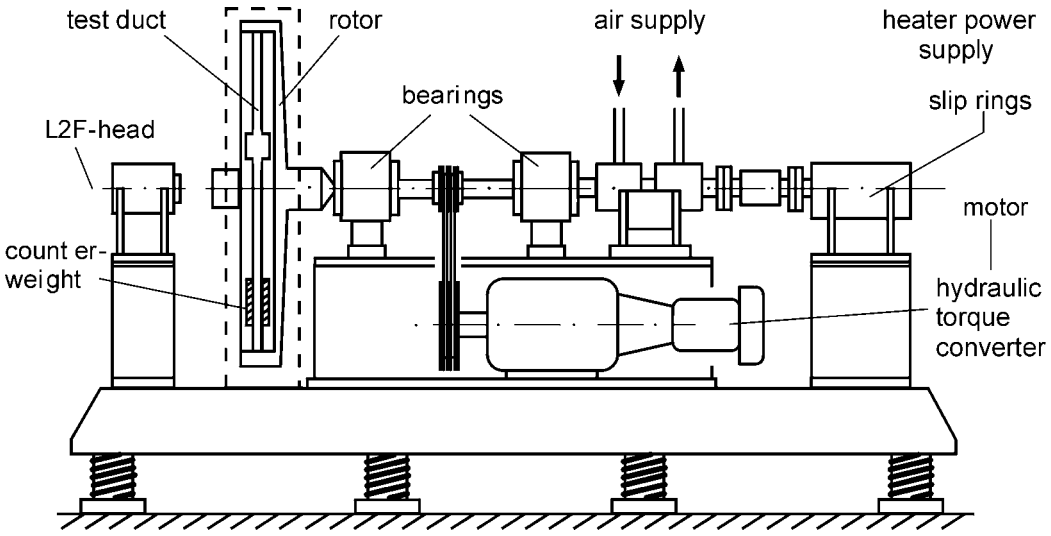

Figure 3: Schematics of the test rig at DLR-Cologne

In Fig. 4 shows a view upon the rotor with inserted test duct with the burst casing being opened. In front of the rotor axis the optical head of the Laser equipment is mounted aligned in the axis with the image rotator prism running at half the speed of the rotor. The rotor has an inner diameter of 1 m and can be driven up to 3.000 rpm.

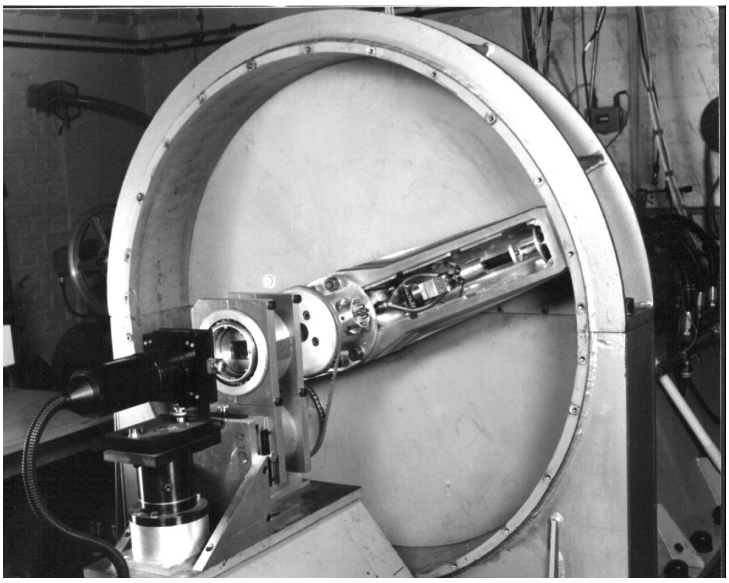

Figure 4: View upon the rotor with inserted test duct and Laser equipment with image rotator prism

The main geometric data of the test duct and the operation conditions are listed below:

Duct diameter	d = 16 mm	Duct length	l = 320 mm
Length-to-diameter ratio	l/d = 20	Eccentricity at mid span	E = e/d = 20
Film cooling hole diameter	d = 2 mm	Hole spacing	s/d = 2
Reynolds number	Re < 100.000	Rotation number	Ro < 0.2
Archimedes number	$Gr/Re^2 < 0.05$		

Flow rate, spin rate, and pressure level can be individually adjusted. The test channel with circular cross-section rotates perpendicular to the axis of rotation with an eccentric orientation. Flow direction in the duct is radially outward. Fig. 5 shows a section through rotor arm with the test duct for Laser measurements mounted.

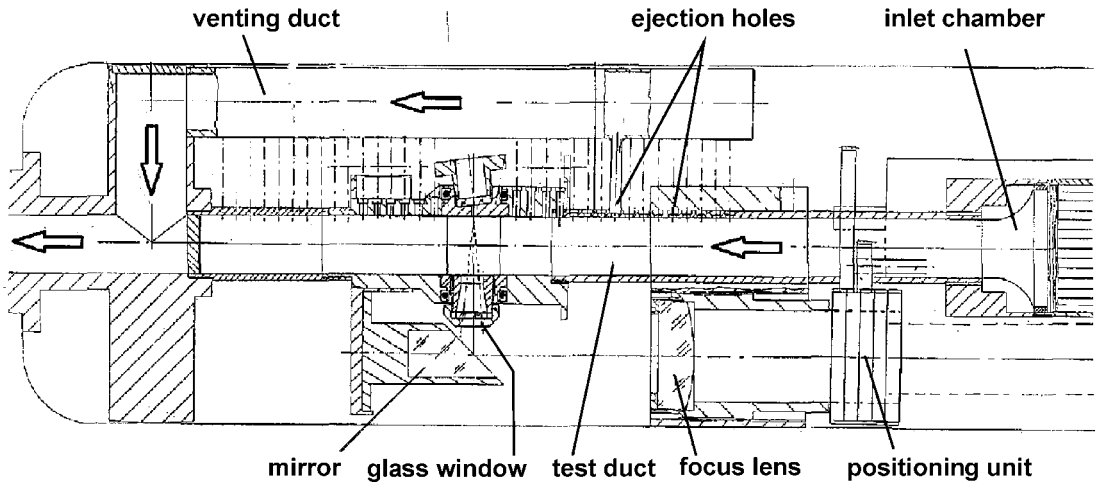

Figure 5: Section through rotor arm with test duct for Laser measurements

The cooling air ejection is simulated by a series of 32 holes of 2 mm in diameter with a typically chosen spacing of s/d = 2. The holes are not open to the environment to ensure that the pressure level opposite the holes is unaffected by changes of the ambient conditions i.e. varying the rotational speed. A collector duct is situated beneath the test duct through which cooling air is vented. Each blowing hole of the test duct is connected to the collector duct via a short straight flexible tube.

Test duct for heat transfer experiments and flow velocimetry

At the Test duct for wall temperature / heat flux investigation, electrical heater foils are fitted to the inner wall to produce a heat flux from the channel to the cooling flow. Two foils are provided to cover the whole duct wall. The duct is constructed with two halves in order to allow access to the inner wall for fixing the foils. The foils itself were manufactured in several layers, a supporting layer of 50 µm thickness, the heater sheet made of constantan material, an insulating layer, a second sheet building the temperature sensor array, and a final smooth protecting layer. Total thickness is given at 150 µm. The heater sheet produces according to the electrical power the same heat power in constant (uniform) wall heat flux mode (UHF). The array of temperature sensors consists of 24 thin film thermocouples of copper-constantan for each duct half (6 in Circumferential direction and 4 in longitudinal direction), 48 measuring points in total. The wall temperatures were evaluated from the thermocouple readings using a previously performed calibration procedure . Fig. 6 shows the layout of the heater/sensor array foil. At the upper side the junctions are intended to electric wiring outside the duct.

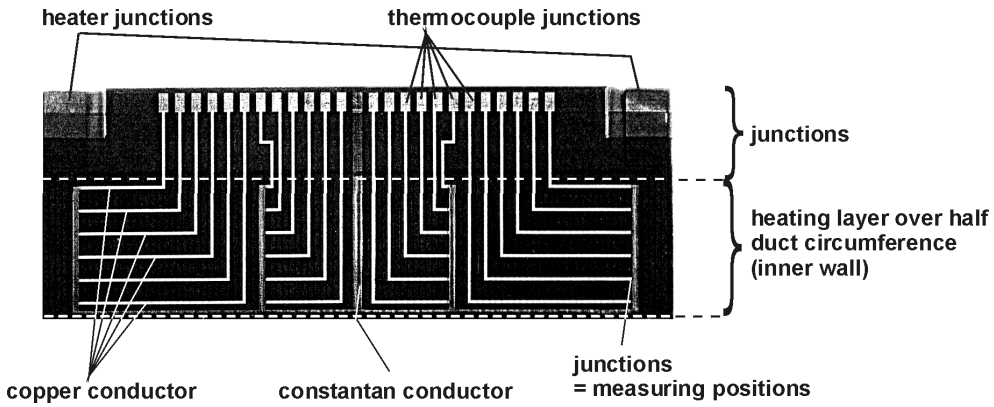

Figure 6: Layout of heater foil with 24 integrated temperature sensors for one duct half

Fig. 7 shows the self adhesive foil with heater and thermocouples in separate layers ready for insertion to one half of the divided duct. After closing the two parts together and sealing, the duct is pre-

pared for drilling of the blowing holes (at the lower edge of the foil in Fig. 6). At the opposite separation joint the electrical connections are performed. The mounted test duct for wall temperature and heat flux measurement shows Fig. 8. The junctions between the ejection holes of the test duct and the collector tube are visible.

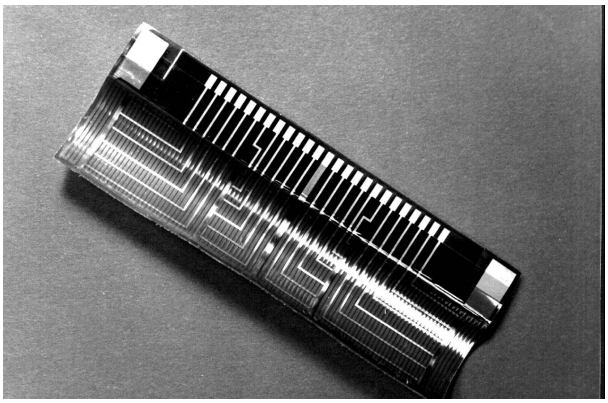

Figure 7: Self adhesive foil with heater and thermocouples in separate layers ready for insertion

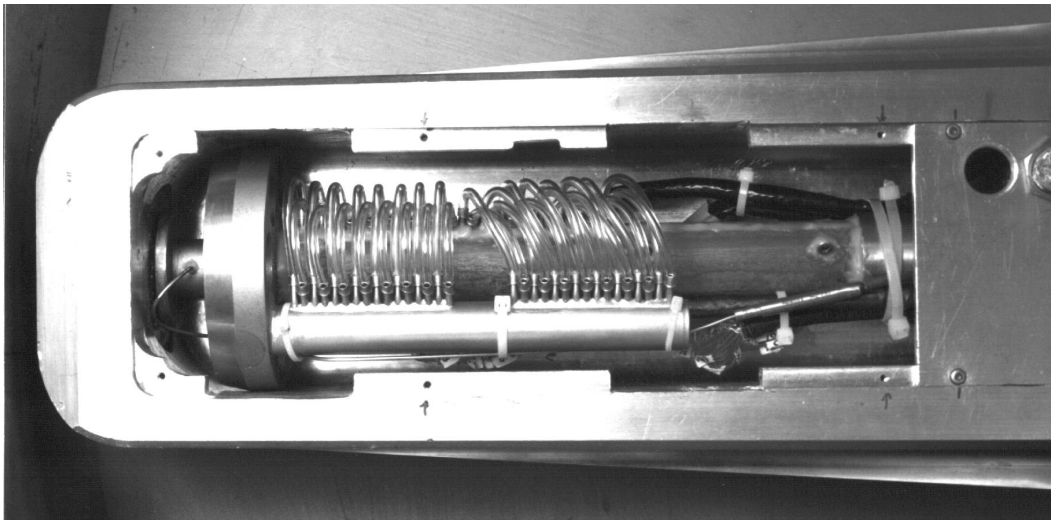

Figure 8: Inserted test duct for temperature measurements in the rotating duct with bleeding

Flow visualization technique

To analyze the rotational flow phenomena in the rotating duct with bleeding off cooling air, a flow visualization technique has been applied. To obtain more information of the vortex behaviour within the cross-section, a co-rotating video system has been installed downstream, viewing inside the duct. A Perspex ring allowed the lighting of a cross-section by a laser light sheet. The laser light is guided into the rotating system via the same optical unit used for the laser flow measurements. In order to visualize the vortex flow structures, seeding of the boundary layer with oil fog is provided by a particle generator. To avoid complete mixing of the oil fog with the air flow, seeding is done a small distance upstream of the observed area via an extra supply line guided through the shaft.
The set-up of the flow visualization technique is shown in fig. 9. The video signal is transferred to a recording system via normal slip rings. With frame grabbing on a PC-machine the video pictures can be captured. The digitized pictures have been improved with regard to luminance and brightness. Although this visualization technique is restricted to laminar flow situation, the main effects are also present and can be studied. Blowing out is made by a series of cooling holes current up the observation cut into the environment.

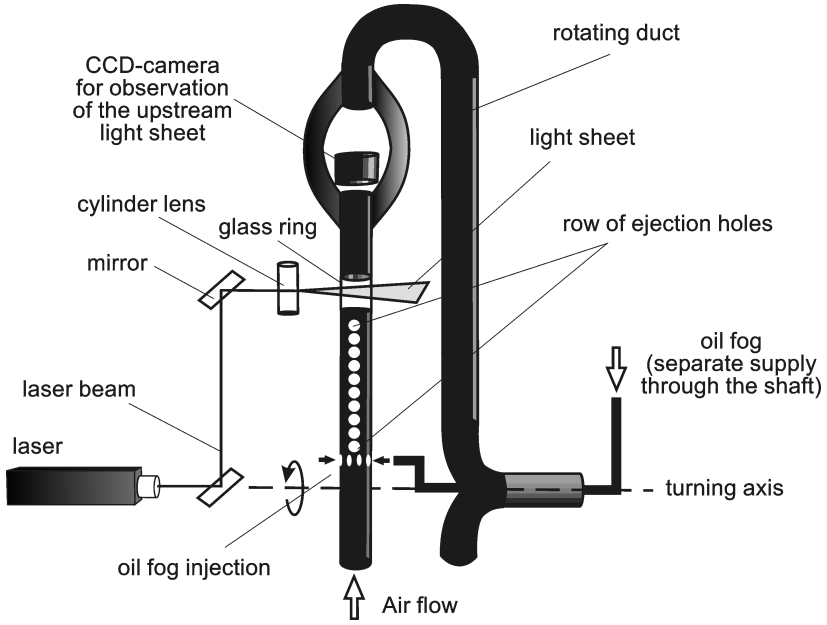

Figure 9: Set-up of vortex flow visualization using a co-rotating camera system and oil fog seeding

Fig. 10 shows the test duct with blowing holes at the left end. At the position where the camera is mounted, the duct splits up into two legs to give place for the camera and insight into the duct. Laterally at the bottom of the duct the cylinder lens for the production of the light sheet, a 90deg-mirror and a focus lens are arranged.

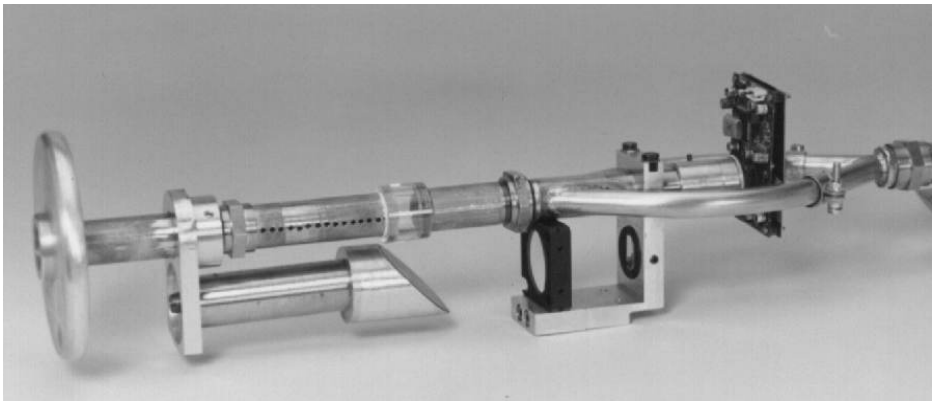

Figure 10: Test duct for visualisation with the camera mounted downstream the lighted cross-section

Flow measurement technique using Laser-2-Focus anemometry

For the non-intrusive measurement of flow velocities, angles and fluctuations inside the rotating duct the Laser 2 Focus (L2F) technique [5,6] has been applied using a own developed optical unit to direct the laser beams into the rotating frame of reference [7]. The optical L2F device mounted in front of the rotor enables the system to stationary non-triggered signal processing. Figure 11 shows a schematic drawing of the optical set-up used in this kind of application.

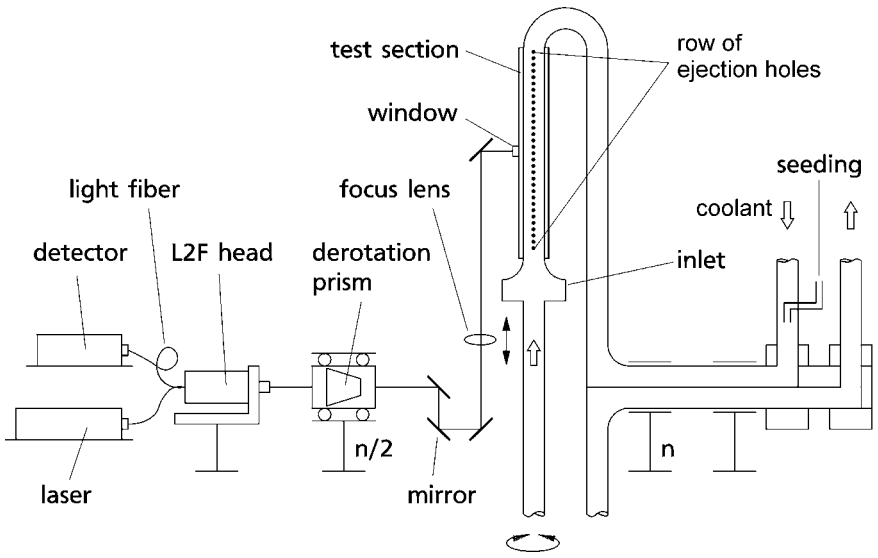

Figure 11: Optical set-up of the laser measuring equipment for the non-intrusive flow measurements

Following the beam path from the laser to the probe volume, the laser light is emitted by an Ar^+ ion laser of 4 Watt power output which is connected to the launching unit mounted to the test rig by an optical fibre for vibration decoupling purpose. In this unit, the laser beam is split into two beams. The rotation prism co-rotating with half the speed of the rotor focuses the two beams in the rotating frame of reference, saving invariable orientation of the light barrier in relation to the rotating duct. From the turning axis the beams are guided by several mirrors to the measuring point inside the duct finally passing a plane optical window in the duct wall. Adjustment of the mirrors enables flow measurements at different circumferential and axial duct locations. The two beams are highly focused in two foci (measuring volume) by means of a traversable focus lens mounted to the rotor. Traversing of the lens, which is also possible during rotation, moves the probe volume within the test section along a radius. Measurements were taken on the opposite half of the duct to avoid influence of the wall shape on the flow near the window. The L2F method is based on time of flight measurements of co-flowing particles. Small oil droplets with a size less than 0.5µm were added to the flow before entering the shaft. The flow-following behaviour of these particles even at high accelerations has been successfully demonstrated and thereby a correlation between particle and flow velocity is assured. The passing of a particle conveyed by the flow through the light barrier (i.e. the 2 foci) produces two consecutive light pulses. The time interval between the signals and the known distance of the foci give the flow velocity. The light pulses received by the same optic in the outer area - the inner part is used for launching the beams - are imaged at two photo multipliers each assigned to a beam in the probe volume. The flow angle is detected by changing the orientation of the light barrier. Due to the 2D-technique and the radial adjustment of the beams, only circumferential flow angle can be measured. In the plane normal to the direction of rotation, where secondary flow is almost parallel to the wall, angle determination produces true flow angle, while in the plane of rotation from suction to pressure side secondary flow is directed normal to the wall. No deviation from the through-flow direction measured in this case confirms the expected line of symmetry in the vortex pattern. For both velocity as well as angle determination, some thousands of time of flight measurements are recorded. The measured data result in frequency distributions from which a statistical mean velocity, degree of turbulence, and flow direction are evaluated. The closest distance to the wall achieved was 0.1 mm.

The test pipe has an inlet settling chamber containing flow straighteners such as impingement plate, honeycombs, and several meshes which should mainly break up incoming vorticity from the upstream conduit where flow is already exposed to rotational forces.

Figure 12 shows the test duct with bleeding tubes interrupted for the optical access at the measuring plane and neighbouring duct for collecting and venting of the cooling air. In the picture, the tubes of the ejection holes are still not connected together.

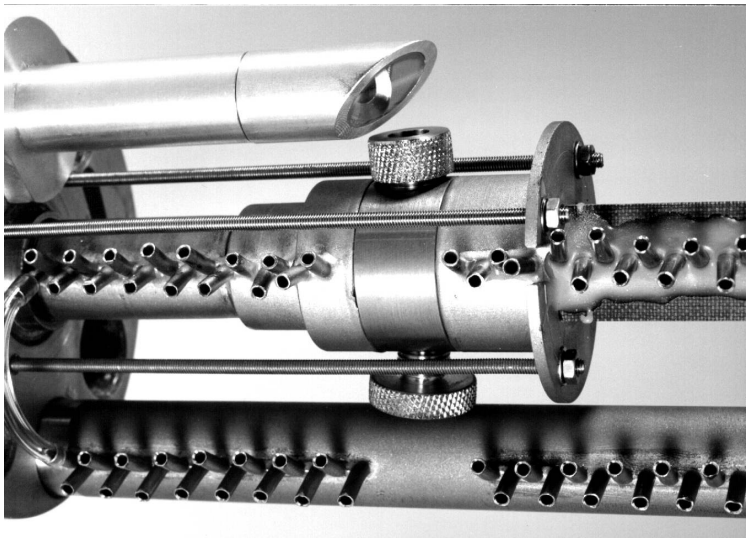

Figure 12: Test duct with bleeding holes and glass window for optical access and venting duct

By varying the position of ejection against the plane of rotation the influence on flow development and vortex structure and intensity is studied. At Fig. 13 the schematic drawing of the Laser measuring plane is given which is fixed to the mid of the duct length. Due to the complexity of the cooling channel with film cooling ejection, measurements were limited to only one measuring plane at half of the duct length.
The experimental uncertainty inherent in the L2F-measurement technique was investigated in detail by Schodl [5]. Among other things it depends on the particle concentration in the measuring volume. In the boundary layer flow the signal rate slows down increasing the signal to noise ratio. Therefore the uncertainties in the velocity and turbulence evaluation are in-between ≤ ±0.5% in the core flow and ±3.0% close to the wall. Angle determination uncertainty ranges between ±0.2° and ±1.0°, respectively. Mass flow rate, heat flux, temperatures, pressures and speed have been measured with an accuracy of ±1%.

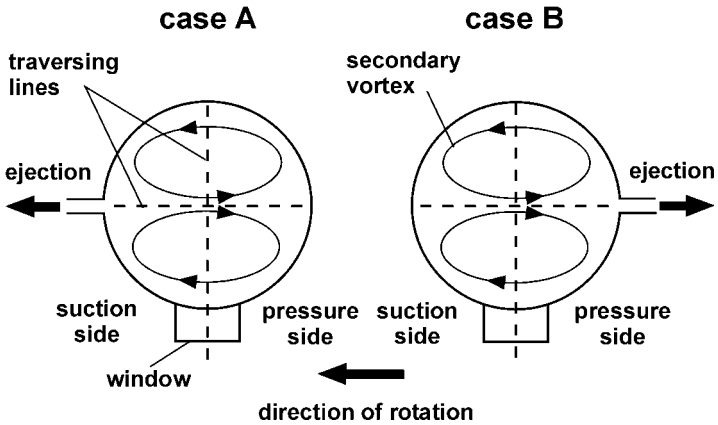

Figure 13: Investigated configurations of ejection at the rotary test duct, pressure side bleeding case A (φ=180 deg) and suction side bleeding, case B (φ=0 deg)

The measuring geometry in relation to the direction of rotation within the cross-section of the duct is described by Fig. 13 where the circumferential angle φ is defined with φ = 0° at the suction side (SS) and φ = 180° at the pressure side (PS). In the following figures radial traversing of the Laser probe volume is done along a line coinciding with the direction of rotation φ = 0 deg and 180 deg and perpendicular to that with φ = 90 deg.

Results from the experiments and discussion

Flow visualization

Depending on the position of cooling air ejection, the secondary vortices in the rotary channel are strongly enhanced in the case where the ejection takes place at the pressure side, and fairly decreased with ejection at the suction side. Fig. 14 shows the structures of the secondary vortices for the two cases.

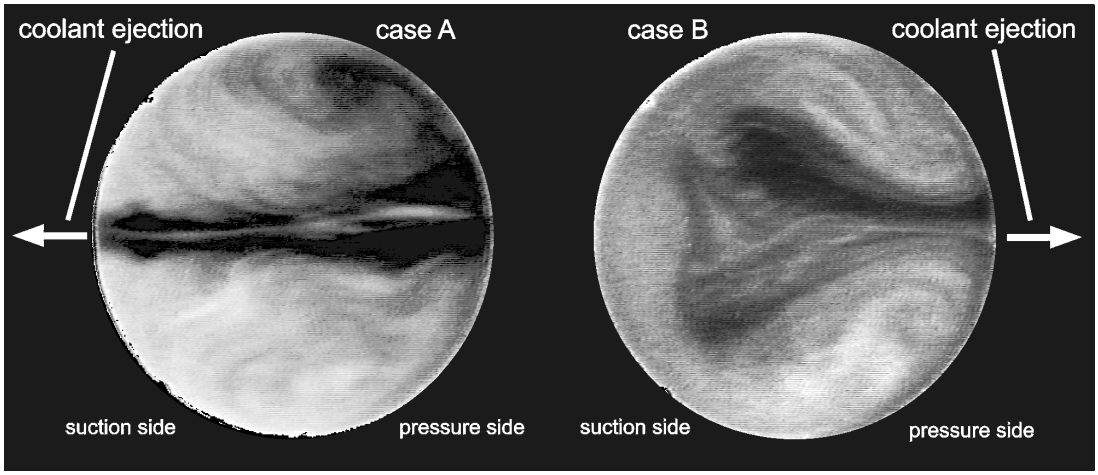

Figure 14: Secondary vortices in the rotating duct with ejection at the suction side case A (left) and at the pressure side case B (right), Ro = 0.04, Re = 500, s/d = 2, m_c/m =0.5

Flow measurements

Depending on the position of ejection the secondary vortices within the rotating duct are strengthened or weakened. Fig. 15 show the measured velocity components u in duct axial direction and v perpendicular to the laser beam direction for suction side ejection (case A) and pressure side ejection (case B). With pressure side ejection a strongly kidney shaped velocity distribution was measured, recognizable at the axial velocity minimum near the center-line of the duct. Likewise the v-component which are in that measuring plane identical with the secondary velocity indicate the presence of strong secondary vortices strengthened by bleeding. The secondary velocities (v) with suction side ejection are quite constant at a low level indicating the presence of only weak vortex motion.

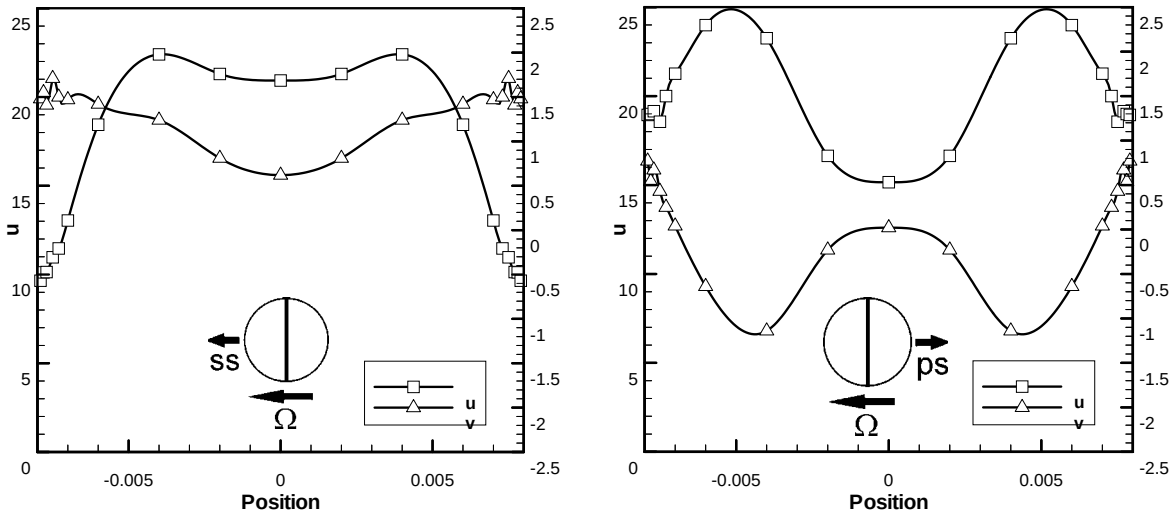

Figure 15: Measured velocity component u , v with suction side ejection (left: φ = 0 deg, case A) and pressure side ejection (right: φ = 180 deg, case B), Re = 60.000, Ro = 0.025)

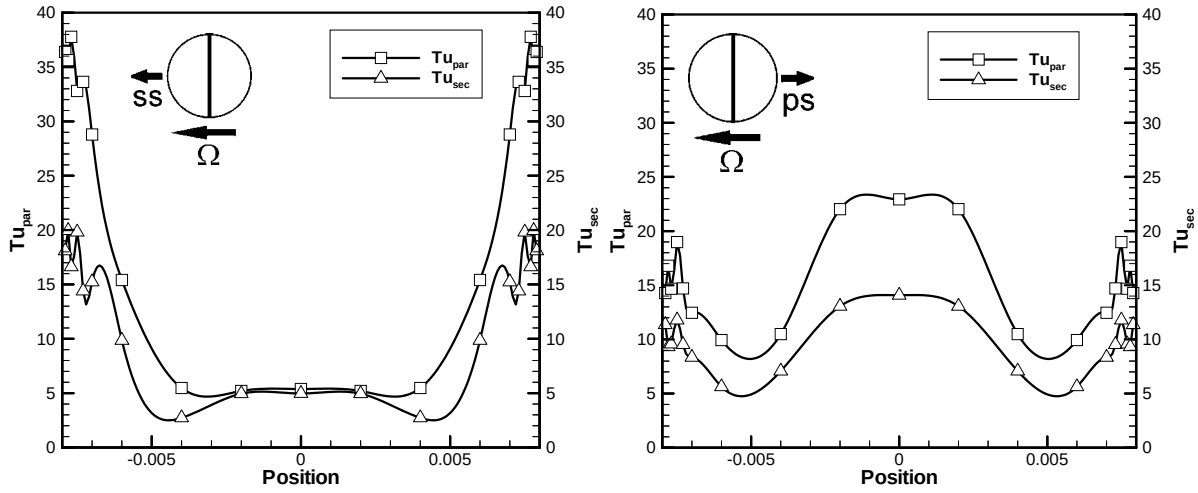

Figure 16: Measured turbulence levels in flow direction (par) and perpendicular (sec) with suction side ejection (left: φ = 0 deg, case A) and pressure side ejection (right: φ = 180 deg, case B), Re = 60.000, Ro = 0.025

Numerical flow prediction

Because of the fact that L2F measurements are difficult in the presented situation of bleeding through a row of holes – the experimental flow investigation was therefor limited to a single measuring plane - a numerical flow analysis would be useful in order to give more precise insight to the flow physics of the whole flow domain. In order to take into account the correct distribution of bleeded mass along the row of holes, both, the test duct and the collecting duct were modelled including the connection tubes. Here, only one result of the performed computations are shown to give an information on the dominant effect of bleeding, i.e. the movement of flow core always to the side where ejection takes place. With suction side ejection the core is displaced to the bleeding row against the usual rotational effect of displacement to the driving wall. No kidney shaped distribution occurs which is known from velocity profiles in rotating ducts without ejection. The adverse effect is observed with pressure side ejection where the rotational effects appear even more enhanced. Fig. 17 show the two computed cases A and B with a Reynolds number of 60.000 and a rotation number of 0.025.

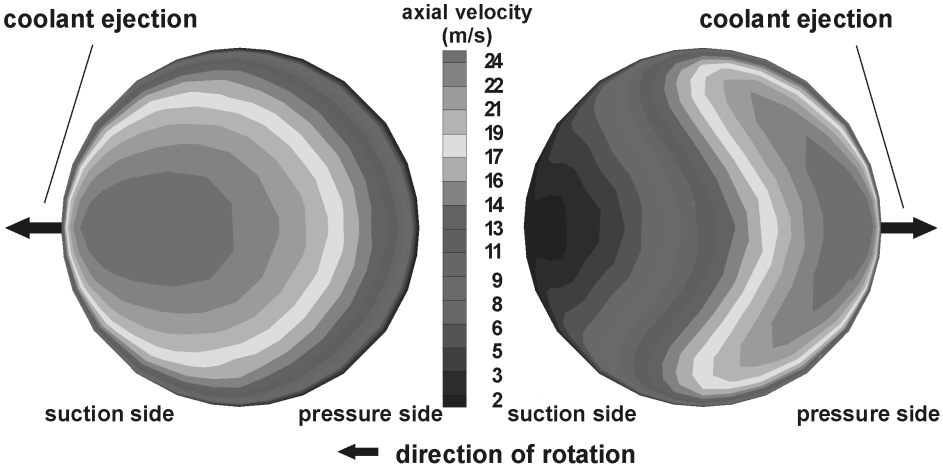

Figure 17: Computed axial velocity distribution with suction side ejection (left: φ = 0 deg, case A) and pressure side ejection (right: φ = 180 deg, case B), Re = 60.000, Ro = 0.025

Wall temperature measurements / heat transfer discussion

The distribution of local wall temperatures are given in Fig. 18 at the different ejection cases. As mentioned previously concerning the strengthening or weakening of secondary motion the corresponding effect is observable with the heat exchange i.e. the temperature distributions. In case B (pressure side

ejection) there appear larger temperature differences than in case A (suction side ejection) due to the action of strong vortices. With pressure side ejection, the movement of the core flow to the ejection holes reduces the velocities at the suction side and diminishes further the velocity gradients at this wall creating big changes in heat transfer rate. With suction side ejection, the movement of the core flow to the ejection holes raises the velocity level at the suction side and enhances the velocity gradients there smoothing out any changes in heat transfer rate. In all measurements a convective proportion of heat exchange within the film cooling holes is visible and, despite badly heat conducting material, unavoidable. It is referred to the represented distributions of wall temperature, that high temperatures indicate a bad heat exchange and low temperatures signify high transfer rates.

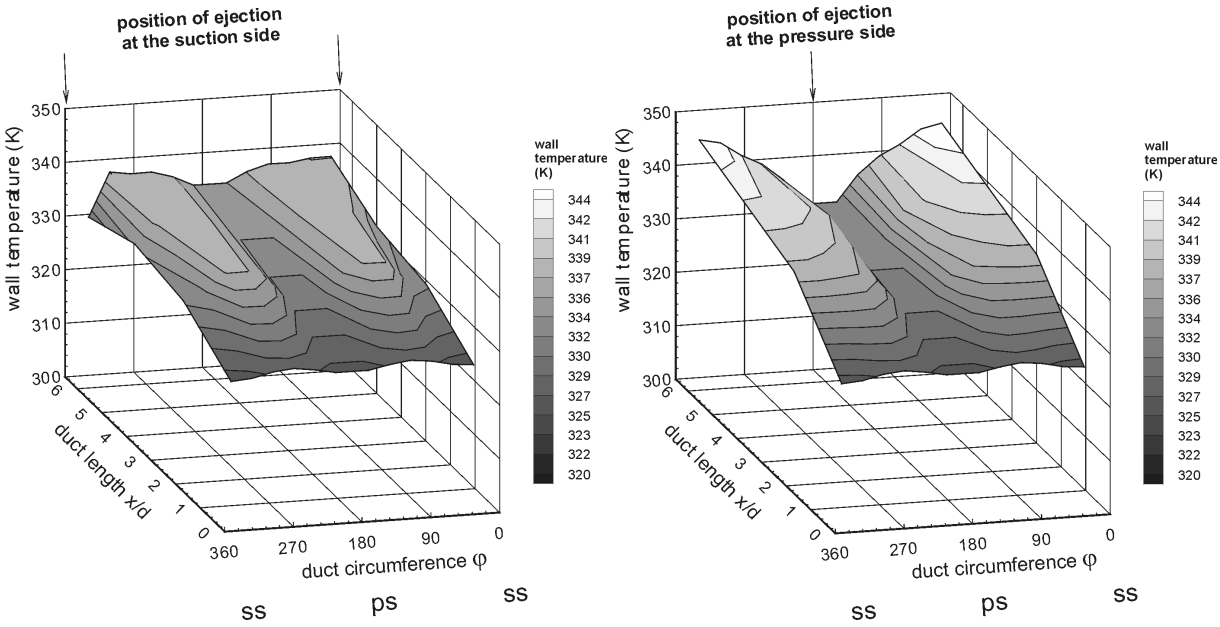

Figure 18: Measured wall temperature distribution with suction side ejection (left: φ = 0 deg, case A) and pressure side ejection (right: φ = 180 deg, case B), Re = 60.000, Ro = 0.025

Conclusions

New experimental data are presented in this paper concerning the influence of rotation as ejection on the flow in a duct rotating in orthogonal mode with radially outward directed flow. From the measurements and the numerical analysis the following phenomena could be stated:

- Flow visualizations of the rotational (isothermal) duct flow verify the presence and magnitude of secondary flow. With the camera technique, it was possible to monitor the vortex behaviour under laminar flow regime. Suction side ejection weakens the secondary vortices (case A) as pressure side ejection strengthens them (case B).
- Non-intrusive flow measurements give precise insights into velocity and turbulence distributions at mid length of the duct. Distortion of axial velocity distribution and the magnitude of secondary velocities arises with pressure side ejection. The kidney-shaped displacement of fluid with higher velocity from the core towards the pressure side leads to drastically diminished shear stresses at the suction side because of the decreased velocity gradients. With suction side ejection, vortex motion is decreased and velocity profiles are smoothed.
- The same effect is observed at the temperature distributions which correspond with heat transfer rate showing big differences in the case of pressure side bleeding.
- Over all, the effect of bleeding is more dominant than the effect of rotation to the flow and heat transfer behaviour.

Acknowledgements

The financial support of AG Turbo, Germany, to this project is gratefully acknowledged. The author wishes to express his gratitude to Dr. R.Schodl and Mr. M.Beversdorff, DLR, for their support in development and application of the L2F measuring system. The helpful support of Mr. H.Hoevel and Mr. M.McNiff, DLR, in preparing and conducting experimental work is equally acknowledged.

References

(1) Berg, H.P., Hennecke, D.K., Elfert, M., Hein, O. (1991). The Effect of Rotation on Local Coolant Side Flow and Heat Transfer in Turbine Blades. *Proc. of the 10th Int. Symp. on Air Breathing Engines (X.ISABE)*, Nottingham, UK, Sept. 1991, 170-183. Also: *ISABE* Paper 91-7016.

(2) Elfert, M. (1994). The Effect of Rotation and Buoyancy on Flow Development in a Rotating Circular Coolant Channel With Radial Inward Flow. in: Measurements in Turbulent Flows. *Experimental Thermal and Fluid Science (ETFS) Journal*, Special issue.

(3) Elfert, M. (1994). The Effect of Rotation and Buoyancy on Radially Inward and Outward Directed Flow in a Rotating Circular Coolant Channel. *49th ATI Congress of Thermotechnic Association of Italy*, 26-30 Sept., Perugia, Italy, Proceedings, 2375-2387.

(4) Elfert, M., Hoevel,H., Towfighi, K. (1996). The Influence of Rotation and Buoyancy on Radially Inward and Outward Directed Flow in a Rotating Circular Coolant Channel. 20*th ICAS Internat. Congress of Aeronautical Sciences*, 8-13 Sept., Sorrento, Italy, Proceedings, 2490-2500, ICAS-Paper ICAS-96-6.10.2.

(5) Schodl, R. (1989). Measurement Techniques in Aerodynamics. *VKI Lecture Series 1989-05*, Von Karman Institute , Brussels, Belgium.

(6) Schodl, R. (1986). Laser-two-focus Velocimetry. in: *Advanced Instrumentation for Aero Engine Components,* AGARD-CP-399, paper 7, Philadelphia, USA.

(7) Beversdorff, M., Hein, O., Schodl, R.. (1992). An L2F-Measurement Device with Image Rotator Prism for Flow Velocity Analysis in Rotating Coolant Channels. *80th Symp.on Heat Transfer and Cooling in Gas Turbines*, AGARD PEP, Antalya, Turkey.

Paper Number: 16

Name of Discusser: B. Simon, MTU Aeroengines Munich

Question:
What happens if air is injected not only either on the pressure or suction side but on both sides.

Answer:
It’s typical for shower head cooling to eject through several rows of holes. But the topic of this project was to analyse the basic effects in a separated manner.

Name of Discusser: K. Jung, Darmstadt University, Germany

Question:
As your cooling duct is closed at the one end, the full cooling air goes through the film- cooling holes. But in a real turbine blade (as I think) not the complete cooling air goes through the film cooling holes. The rest passes a u-bend or a multipass-system. Therefore the ratio between the velocities in the cooling holes and the feeding duct is changed. Could you say something to the influence of a change in this ratio?

Answer:
We have investigated only the case with closed end at the duct where all of coolant mass is ejected via the cooling ejection holes.
Connection of a U-turn or multipass-system leads to an unpredictable ratio of bleeded mass and the proportion remaining in the cooling system and it is not used in practise as far as I know.

Name of Discusser: S. Wolff, Universität der Bundeswehr Munich

Question:
What is about the discharge coefficient due to the vortex structure?

Answer:
Due to limitation to one measuring plane for flow measurement, no information is available regarding the discharge coefficient.
However the cross-section area of the duct is two times bigger than the sum of the area of all holes, so uniform discharge should be expected.